

Statistical dynamical validity of a Jahn-Teller model for TI^+ luminescence

A. Ranfagni, D. Mugnai, P. Fabeni, and G. P. Pazzi

Istituto di Fisica Applicata "Nello Carrara" CNR, Via Panciatichi 64, 50127 Firenze, Italy

(Received 25 March 2002; revised manuscript received 5 July 2002; published 21 November 2002)

The old problem of the interpretation of the emission properties of TI^+ centers in alkali halides is reconsidered in the light of recent experimental evidence relative to anomalous decay in the slow-emission component. A plausible interpretation, based on the Jahn-Teller model in its simpler version, is proposed, considering the statistical dependence on the ensemble of the luminescence centers and the concurrent effect of the dynamical relaxation of the lattice.

DOI: 10.1103/PhysRevB.66.184107

PACS number(s): 71.70.Ej, 71.55.-i, 63.20.Mt

The emission properties of TI^+ -like impurity centers in alkali-halide crystals is an old and fascinating problem, to the solution of which many efforts have been devoted since the 1960s and even much before.¹ A definite improvement in our understanding of this subject was made thanks to a model based on the Jahn-Teller effect as developed by Fukuda in 1970.² This model is based on the assumption of the coexistence of two kinds of minima on the ${}^3T_{1u}$ and ${}^3A_{1u}$ excited-state adiabatic potential surfaces (electronic configuration $a_{1g}t_{1u}$) in the space of the normal coordinates of the quasimolecules which constitute the luminescence centers. The two emission bands (A_T and A_X) are considered to be due to transitions from these minima to the ground state ${}^1A_{1g}$ (electronic configuration a_{1g}^2).

The Fukuda model was subsequently modified, as described in a number of papers.³ In particular, it was demonstrated that the coexistence is due to the quadratic Jahn-Teller effect and/or anharmonic terms, or to strong spin-orbit mixing between ${}^3T_{1u}$ and ${}^1T_{1u}$ states. The level scheme resulting from spin-orbit mixing appears to be particularly suitable to explain TI^+ emission, while the higher-order electron-lattice interactions seem the most likely agent to produce coexistence in lighter impurities.

The subject continued to represent an interesting field of research as demonstrated by works appearing in the literature.⁴ More recently, an interpretation of the anomalous decay in the slow-emission component observed in several cases has been proposed on the basis of an original and suggestive mechanism.⁵ This is based on the assumption that the lattice relaxes at the same time scale (ms) as the slow-component decay time.⁶

The purpose of the present work is twofold. First, in light of more recent results, we wish to test the Jahn-Teller model in a more quantitative fashion than was made a few decades ago. Second, we propose a possible interpretation of the anomalous slow component, not in contradiction to the one of Ref. 5, but as a plausible alternative, still based on the Jahn-Teller effect and its statistical dependence on the ensemble of luminescence centers, concurrent with the dynamical relaxation of the lattice.

We focus attention on TI^+ centers, namely, $\text{KX}:\text{TI}^+$ ($X = \text{I, Br, Cl}$), which are the cases most widely studied. In addition, due to its strong spin-orbit interaction, TI^+ can be treated on the basis of a simplified Jahn-Teller model, as was early proposed, by modifying that of Fukuda, since 1972.⁷

The Jahn-Teller effect we are considering is limited to the ε_g subspace of tetragonal distortions and to the linear terms of the electron-lattice interaction. In Ref. 7 the potential surfaces are obtained by diagonalizing the electron-lattice interaction matrix, taking into account the spin-orbit interaction and the lattice potential energy.

As anticipated before, the Jahn-Teller model is based on the coexistence of two kinds of minima on the ${}^3T_{1u}$ relaxed excited state, in the space of normal coordinates of the $(\text{TX}_6)^{5-}$ cluster. These minima, accessible after optical absorption in the A band, lead to the A_T and A_X emission bands. In the framework of the linear Jahn-Teller effect, within the ε_g subspace of tetragonal distortions (Q_2, Q_3), the coexistence is allowed by the strong spin-orbit mixing between the triplet ${}^3T_{1u}$ and the singlet ${}^1T_{1u}$ states, from which originates the ${}^3T_{1u}^*$ and ${}^1T_{1u}^*$ states.⁸ The minima from which the A_T emission originates are the tetragonal $T_{x,y,z}^*$ minima which are mainly constituted by the singlet state ${}^1T_{1u}$ (see Fig. 1). The emission A_X originates from minima of different symmetry: three couples of nearly tetragonal quasidegenerate X minima,⁹ which can become symmetrically different if the relative coordinates (τ_{2g} subspace) are included; this aspect is not considered in the present treatment.³ Therefore, as anticipated before, we limit our analysis to the subspace of tetragonal coordinates.

For our purposes, it is sufficient to vary only the tetragonal coordinate Q_3 , taking $Q_2 = 0$. By referring the zero energy to $W_0 - G$ (W_0 is the energy difference between the excited state $a_{1g}t_{1u}$ and the ground state a_{1g}^2 electronic configuration, and G is the exchange integral) the energy levels $E(Q_3)$ were obtained by solving a third-degree secular equation. By putting $y = E/\xi$ (ξ being the spin-orbit coupling constant) and $x \equiv x_3 = (-b/2\sqrt{3}\xi)Q_3$, the cross section of the ${}^3T_{1u,z}^*$ adiabatic potential-energy surface is given by⁷

$$y = -x - \frac{1}{4} + g - [(3x - \frac{1}{4} - g)^2 + \frac{1}{2}]^{1/2} + Ax^2, \quad (1)$$

where $g = G/\xi$ is the ratio of the exchange integral to ξ , $A = 12(1 - \beta)\xi/b^2$, β is a quadratic term—the only one considered in this model—which accounts for the difference in curvature between the ground- and the excited-state potential surfaces, and b is the electron-lattice coupling constant for the tetragonal modes. In this way, the model is found to be dependent only on the two dimensionless parameters, A and g . In spite of the approximation involved, this greatly facili-

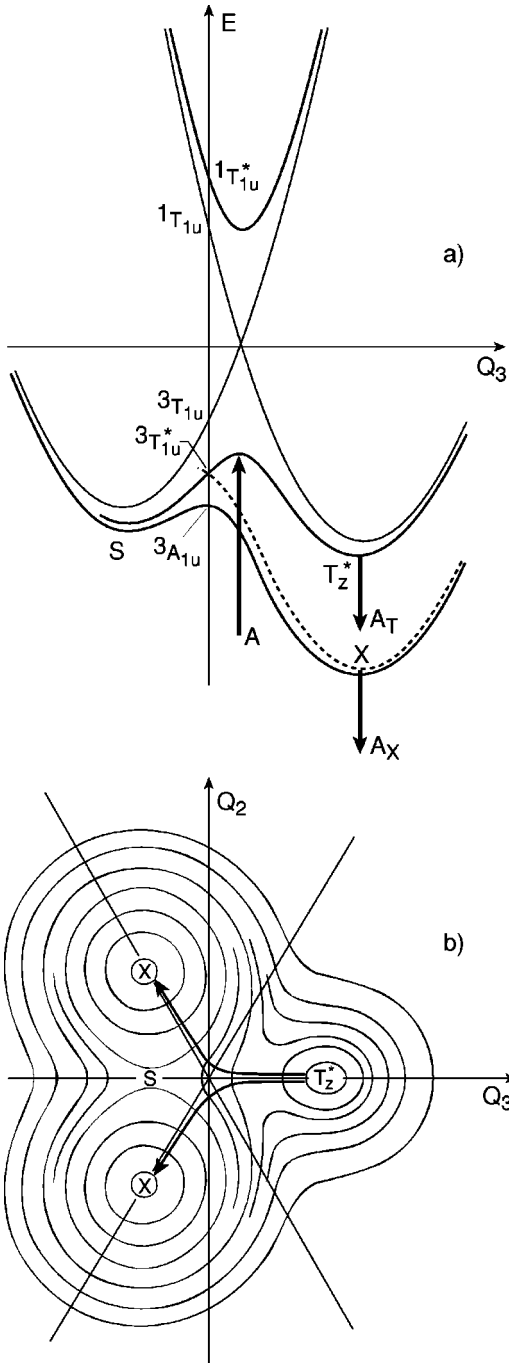


FIG. 1. Excited states relative to the electronic configuration $a_{1g}^4 t_{1u}$ involved in the A -absorption band and A_T and A_X emissions. In (a) we have, along the Q_3 axis, the cross sections of the $^1T_{1u}$ and $^3T_{1u}$ states (thin lines) from which originate, by means of spin-orbit coupling, the $^3T_{1u}^*$ and $^1T_{1u}^*$ states, whose component z is represented by heavy lines. The dashed line represents the cross sections of x and y components. The underlying $^3A_{1u}$ state is the trap level. Arrows indicate the absorption and emission transitions. In (b) we represent the map of the $^3T_{1u,z}^*$ potential surface, in the Q_2, Q_3 subspace of the tetragonal coordinates, showing the coexistence of two equivalent X nearly tetragonal minima (S is a saddle point between them) with a higher-lying T_z^* minimum. The heavy lines represent the least action paths for the nonradiative transitions from T_z^* to X minima. The map of the $^3T_{1u,x(y)}^*$ potential surfaces are equivalent but rotated by $\pm 2\pi/3$, in the Q_2, Q_3 space, after Ref. 7.

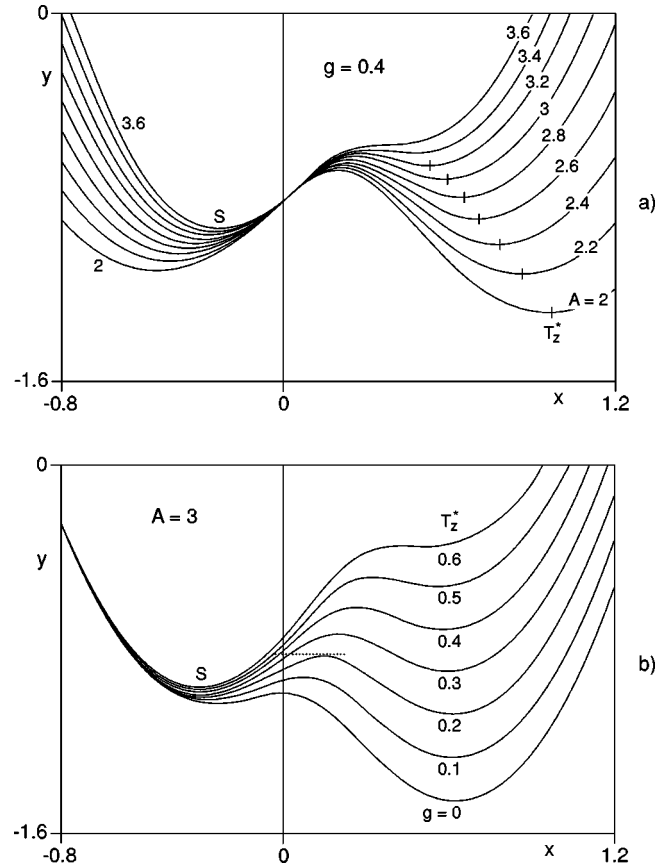


FIG. 2. Cross section along the Q_3 coordinate ($Q_2=0$) of the $^3T_{1u,z}^*$ potential surface, as given by Eq. (1). In (a) we report the computations obtained for $g=0.4$ and for some values of the parameter A which range from 2 to 3.6. The positions of the T_z^* minimum are marked: they strongly increase by lowering A . The point S is the saddle point between two rhombic minima X . In (b) we report the results obtained for $A=3$ and by varying g from zero (which represents the cross section of the $^3A_{1u}$ trap level) to 0.6, which is the limiting value for the existence of the T_z^* minimum, whose position is almost independent from g .

ties the test in a comparison with the experimental results. More sophisticated schemes, such as those modeled on the basis of second-order Jahn-Teller terms (namely, all those of the type $a_{\epsilon\epsilon} Q_{\epsilon}^2$), or similar (such as $c_{\epsilon\tau} Q_{\epsilon} Q_{\tau}$), necessitate the inclusion of a great number of parameters, which makes serious quantitative testing extremely difficult.³ In Fig. 2, we report some cross sections of y computed by Eq. (1) for some typical values of the parameters. In the Fig. 2(a), we took $g=0.4$ and we varied A in the 2–3.6 range, while in the lower part [Fig. 2(b)] we took $A=3$ and we varied g in the 0–0.6 range. For $g=0$, Eq. (1) gives the cross section of the potential surface relative to the $^3A_{1u}$ trap level underlying the $^3T_{1u}$ transition-allowed level. This representation allows us to make a first, preliminary, selection of the parameter values relative to the different cases of Tl^+ phosphors, as can be seen from the data reported in Table I.

A more refined selection will be made later after some important corrections have been made by considering the dependence of the mixing with the $^1T_{1u}$ state, which is the

TABLE I. Estimate of the A and g parameter values from the available experimental data of G , ξ , b^2 , and trap depth for TI^+ impurities in KI, KBr, and KCl crystals (Ref. 16), under the assumption that $\beta=0.66$. The last column reports the values of A as determined by WKB analysis (Ref. 11) of the nonradiative transition rate assuming $g=0.4$ and $\tau=25$ ns.

Phosphors	Emission (eV)	Trap depth (meV)	G (eV)	ξ (eV)	b^2 (eV)	g	A ($\beta=0.66$)	A_{WKB} ($g=0.4$)
KI: TI^+	$\begin{cases} A_T:3.70 \\ A_X:2.89 \end{cases}$	$\begin{cases} 46-55 \end{cases}$	0.16	0.51	0.64	0.31	3.2	3
KBr: TI^+	$\begin{cases} A_T:4.02 \\ A_X:3.50 \end{cases}$	$\begin{cases} 60 \\ 40 \end{cases}$	0.23	0.60	0.79	0.38	3.04	2.8
KCl: TI^+	$\begin{cases} A_T:4.17 \\ A_X:2.61 \end{cases}$	$\begin{cases} 32-56 \end{cases}$	0.28	0.69	0.92	0.56	3	~ 2.9

only one allowed for the absorption transition from the $^1A_{1g}$ ground state. A consideration of this fact has led to the deduction that the point of arrival of the transition at the excited state, $^3T_{1u}^*$, is shifted from $x=0$ toward a point where $x>0$. The amount of this shift has been estimated to be of the order of $(\hbar\omega/A\xi)^{1/2}$, where $\hbar\omega$ is the vibrational quantum in the well of the T_z^* minimum.¹⁰ Thus, according to the parameter values of Table I, we have a shift of about $\Delta x=0.1-0.2$. In inspecting Fig. 2, we note that this shift is comparable with (or is behind) the position of the maximum of the barrier between the T_z^* minimum and the saddle point S (situated between the X minima which are dislocated at positions with $Q_2 \neq 0$ not visible in Fig. 2, which was obtained for $Q_2=0$ ^{3,7}). This fact explains why the system, after absorption at a low temperature, relaxes preferentially into the tetragonal minimum T_z^* , while the lower-lying X minima are less populated, with a consequent weaker intensity of the A_X emission with respect to the A_T one. By increasing the temperature, the population of the X minima is augmented at the expenses of the population of the T_z^* minimum, by means of nonradiative transitions from the well of the T_z^* minimum, the probability of which increases with the temperature. In this way, it was possible to account for the intensity balance of the two emissions. By using a WKB treatment of the problem,¹¹ it was possible to obtain an accurate description of the intensity balance for KI: TI^+ and KBr: TI^+ , and to better discriminate values for the parameter A in a narrow interval of values: 3 and 2.8, for KI and KBr, respectively. For KCl, the situation is less clear since it is not definitely accepted that there is an A_X emission or, rather, the A_T one (at 305 nm), which has to be considered to be doubled.¹² However, from the temperature dependence of the intensity and decay time of an emission at 475 nm, we can argue that this emission presents many characteristics of an A_X emission.¹³ On this assumption, we can argue that parameter A , which fits the temperature dependence of the emission intensity, should again be comparable with the previously obtained values, perhaps intermediate, say, ~ 2.9 . The temperature Θ at which the A_T and A_X emission intensities become comparable can be estimated by the relation $\nu \exp(-E_T/k\Theta) \approx \tau^{-1}$, where ν is the vibrational frequency within the T_z^* well, E_T is the height of the barrier, and τ is the

radiative lifetime of the A_T emission. A more accurate analysis has been performed by evaluating the nonradiative transition probability including tunneling and thermally overcoming the barrier. The quantity which determines the transition probability is the transmission coefficient which, in turn, is dependent on the action integral across the barrier.¹¹ The quantity reported in Fig. 3, multiplied by $2\xi A^{1/2}/\hbar\omega$, gives the action S/\hbar as a function of the energy $\Delta E/\xi$, calculated for some values of the parameter A in a range of values of interest for us. In the same figure, the dotted lines represent the loci of the decay time, for nonradiative transitions from the T_z^* well, obtained as $\tau_d=(D\nu)^{-1}$, where $D=[1+\exp(2S/\hbar)]^{-1}$ is the transmission coefficient. We note that τ_d is extremely sensitive to the parameter values, and

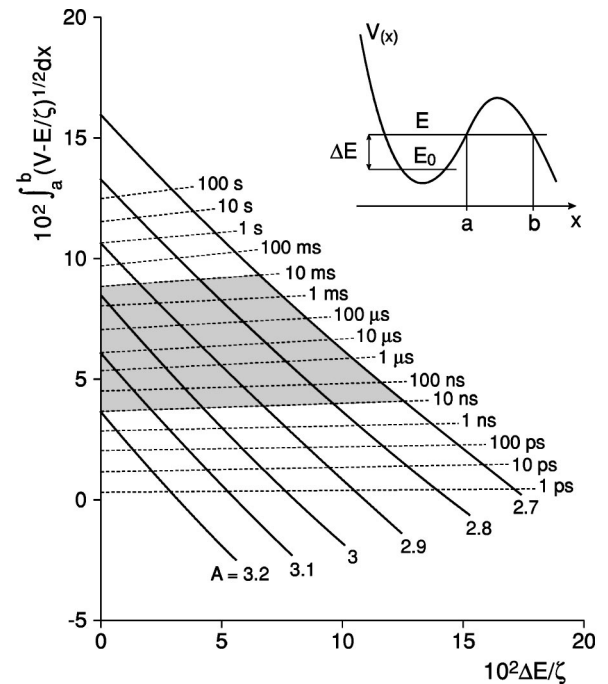


FIG. 3. Action integral, in units of $\xi A^{1/2}/\hbar\omega$, along the classical path as a function of the energy, with $E_0/\xi=1.25 \times 10^{-2}$, $g=0.4$, and $A=2.7-3.2$. The dotted lines are the loci of decay-time values. The shaded area, comprised between 10 ns and 10 ms, is of interest for an interpretation of the anomalous decay of the luminescence.

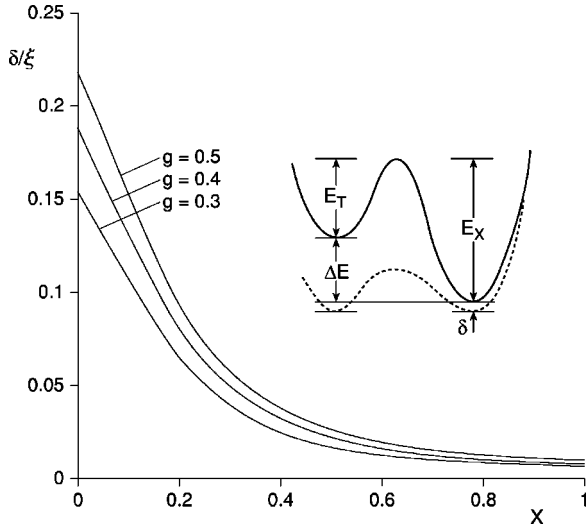


FIG. 4. Trap depth δ/ξ as given by the energy difference between the cross section of the ${}^3T_{1u,x(y)}^*$ potential surface, the lowest solution of Eq. (2), and the cross section of the ${}^3A_{1u}$ potential surface, Eq. (1) for $g=0$, as a function of the coordinate x , and for $g = 0.3, 0.4$, and 0.5 . In the inset, a sketch of the potential surface of the ${}^3T_{1u,z}^*$ state, with the underlying trap level ${}^3A_{1u}$, appears along one of the transition paths of Fig. 2.

can vary from picoseconds to tens of seconds. The range of values of interest for us is the one comprised between 10 ns and 10 ms, since this one is just the range of variation of decay times observed in the emission bands.⁵ In other words, we assume that, due to the crossing of the barrier, the delay time is at the origin of the anomalous behavior of the emission bands, or at least strongly contributes to it. The anomaly consists of a gradual change in the decay time, from the fast component (~ 10 ns) to the slow one (~ 10 ms), by assuming all the intermediate values over a span of time of several ms.⁵ It may be argued that this mechanism can explain only the anomaly of the slow-component of the A_X emission, the minima (X) of which are the ones mainly populated by non-radiative transitions from the T^* wells. However, a consideration of the (important) role of the trap level ${}^3A_{1u}$ (responsible for the slow component) underlying the allowed level ${}^3T_{1u}^*$, as well as of back tunneling from X to T^* wells,¹⁴ makes the role of the above-analyzed nonradiative transitions relevant even for the slow component of the A_T emission (still in the scale of ms). This slow component, which was discovered only recently (while before it was considered nonexistent¹²), is indeed considerably weaker than the one of the A_X emission.⁴ This supports our hypothesis of a second-order mechanism (the first is the nonradiative transitions from T^* to X minima analyzed above; the second is the one relative to relaxation into the trap level). The resulting level scheme (essentially a three-level one) is depicted in the inset of Fig. 4. This scheme is very similar to the one derived in Ref. 4, even if there a four-level model was considered. However, the difference in height of different minima on the ${}^3A_{1u}$ trap level (~ 10 meV) has to be considered unimportant with respect to the other quantities.

As for the gradual change in the decay time, which would require using the sum of several exponential functions with different lifetimes that range over several orders of magnitude,⁵ two explanations are conceivable within the framework of the present model: one is based on a dynamical effect, the other, on a statistical effect.

(i) In adopting the same mechanism proposed in Ref. 5, we find that a slow response of the lattice to the Jahn-Teller local distortion of the $(\text{TLX}_6)^{5-}$ centers makes it possible to obtain a different equilibrium coordinate, the one of the T_z^* minimum in Fig. 2, increasing in temporal succession. This, in turn, can be seen as a gradual change in parameter A , i.e., a lowering, with a consequent variation in the decay time according to Fig. 3.

(ii) Alternatively, we can hypothesize that, in the ensemble of $(\text{TLX}_6)^{5-}$ centers, we have a distribution of possibilities for the equilibrium coordinate in the excited state, after absorption and relaxation to the equilibrium configuration, with both of these latter processes being considered practically instantaneous (ps).

These two mechanisms are to be considered not in contradiction; rather, a combination of both is more probable. One advantage, in the case of item (i) with respect to the model of Ref. 5, is that it is not necessary for the lattice relaxation to occur within the same range of time of the emission (ms); a much shorter one is sufficient (say, μs), since even a small further variation in the equilibrium produces a strong increase in the time (delay-time amplification).

We are now in a position to improve our determination of the parameter values which characterize the different cases. To this end it is useful to evaluate the energy difference (trap depth δ) between the X minima and the underlying trap level. The cross sections of the ${}^3T_{1u,x}^*$ and ${}^3T_{1u,y}^*$ states are given by $y = \bar{y} + Ax^2$, where \bar{y} is given by the lowest solution of the equation, obtained in the same framework which supplies Eq. (1),⁷

$$\bar{y}^3 - 2g\bar{y}^2 - \bar{y}\left(12x^2 + 4gx + \frac{3}{4}\right) + g\left(16x^2 + \frac{1}{2}\right) + 16x^3 + \frac{1}{4} = 0. \quad (2)$$

The cross section of the ${}^3A_{1u}$ trap level is given, we recall, by Eq. (1) for $g=0$. In Fig. 4 we report the quantity δ/ξ calculated by Eqs. (1) and (2) as a function of coordinate x for some values of g . The resulting curves, which are independent from parameter A , clearly show a marked reduction in the trap depth with an increase in the configuration coordinate. From a knowledge of the trap depth in the minimum, we can determine the corresponding coordinate value. This, for both minima T_z^* and X , is given by the approximate relation $x_0 \approx 2/A$, while it is practically independent of g (see Fig. 2 for a better determination). In this way, we can arrive at a determination of A or, inversely, from a knowledge of A , at the trap depth. The same criterion can also be applied for the energy separation of the T_z^* minimum with respect to the trap level, $\Delta E + \delta$ in the inset of Fig. 4. Also in this case, the energy separation in the minimum is strongly dependent on

TABLE II. Alternative estimation of the A and g parameter values and trap depth taking into account the shift of the point of arrival, at $x > 0$, of the A -absorption transition, the inversion temperature Θ_i of the emission A_T and A_X (Refs. 11 and 13), and the vibrational quantum $\hbar\omega$ (Ref. 17); $\tau = 2.5 \times 10^{-8}$ s and $1 - \beta$ is given by $b^2/6x_0\xi$.

Phosphors	$\hbar\omega$ (cm^{-1})	ν (10^{12} Hz)	Θ_i (K)	$E_T = k\Theta_i \ln(\tau\nu)$ (meV)	A_{eff}	g_{eff}	x_0	$(1 - \beta)$	
KI:Ti ⁺	96	2.86	~ 40	38.5	$\left\{ \begin{array}{l} \Delta E = 178 \\ \delta = 10 \end{array} \right.$	3.75	0.175	0.45	0.46
KBr:Ti ⁺	116	3.47	~ 80	78.4	$\left\{ \begin{array}{l} \Delta E = 264 \\ \delta = 12 \end{array} \right.$	3.35	0.22	0.53	0.41
KCl:Ti ⁺	144	4.30	~ 70	69.0	$\left\{ \begin{array}{l} \Delta E = 345 \\ \delta = 17 \end{array} \right.$	3.55	0.25	0.49	0.45

the minimum coordinate value, and decreases while x_0 increases¹⁵ or, if we prefer, with a lowering of A , which produces deeper minima (see Fig. 2). By taking into account the shift in the point of arrival in the absorption process mentioned at the beginning, we have that the value of g as deduced by the peak absorption band is overestimated, because the shifted point of arrival corresponds, for $x=0$, to a curve with a higher value for g . In fact, the value of G , as deduced by peak absorption-band values, considered to be peaked at $x=0$, gives a value for $g=G/\xi$ (assuming ξ unvaried) nearly twice that relative to the curve which has its maximum (for $x > 0$) at the same energy value [see, in Fig. 2(b), the dotted line linking the curves obtained for $g=0.2$

and $g=0.4$]. This produces nearly a halving of g and a consequent depression of the T_z^* minimum. On the basis of these criteria, we arrive at the determinations reported in Table II, which can be considered as a rather accurate determination of the parameter values.

It seems therefore safe to conclude that the present model appears to be more suitable for interpreting the complex phenomenology of these kinds of luminescence centers, at least in the case of Ti⁺ impurity. Moreover, we can argue that similar conclusions can be drawn also for other cases, especially those with strong spin-orbit interaction.

The authors enjoyed stimulating and useful discussions with L.S. Schulman, E. Mihóková, and M. Nikl.

¹See W.B. Fowler, in *Physics of Color Centers*, edited by W.B. Fowler (Academic, New York, 1968).

²A. Fukuda, Phys. Rev. B **1**, 4161 (1970).

³A. Ranfagni, D. Mugnai, M. Bacci, G. Viliani, and M.P. Fontana, Adv. Phys. **32**, 823 (1983).

⁴An important contribution can be found in J. Hlinka, E. Mihóková, M. Nikl, K. Polák, and J. Rosa, Phys. Status Solidi B **175**, 523 (1993).

⁵B. Gaveau, E. Mihóková, M. Nikl, K. Polák, and L.S. Schulman, Phys. Rev. B **58**, 6938 (1998); J. Lumin. **92**, 311 (2001).

⁶L. S. Schulman, E. Mihóková, A. Scardicchio, P. Facchi, M. Nikl, K. Polák, and B. Gaveau, Phys. Rev. Lett. **88**, 224101 (2002).

⁷A. Ranfagni, Phys. Rev. Lett. **28**, 743 (1972); A. Ranfagni and G. Viliani, J. Phys. Chem. Solids **35**, 25 (1974).

⁸Because of the spin-orbit mixing the ${}^3T_{1u}$ and ${}^1T_{1u}$ states are replaced by the linear combinations ${}^3T_{1u}^* = \mu({}^3T_{1u}) - \nu({}^1T_{1u})$ and ${}^1T_{1u}^* = \nu({}^3T_{1u}) + \mu({}^1T_{1u})$, where the mixing coefficients μ and ν are dependent on the configuration coordinate (Ref. 7).

⁹Minima on the potential surfaces exist at configurations slightly lower than tetragonal due to the spin-orbit interaction: for this reason they are named nearly tetragonal (sometimes called

rhombic, see Ref. 2, p. 4169). These six minima are labeled X and constitute three couples of nearly degenerate minima.

¹⁰D. Mugnai, A. Ranfagni, and G. Viliani, Phys. Rev. B **25**, 4284 (1982).

¹¹A. Ranfagni, G. Viliani, M. Cetica, and G. Molesini, Phys. Rev. B **16**, 890 (1977).

¹²R. Illingworth, Phys. Rev. **136**, A508 (1964).

¹³A. Ranfagni, G.P. Pazzi, P. Fabeni, G. Viliani, and M.P. Fontana, Phys. Rev. Lett. **28**, 1035 (1972); M. Bacci, P. Fabeni, M.P. Fontana, G.P. Pazzi, A. Ranfagni, and G. Viliani, Alta Freq. **44**, 267 (1975).

¹⁴A. Agresti, D. Mugnai, A. Ranfagni, and R. Englman, Phys. Rev. B **28**, 4307 (1983).

¹⁵This tendency is indeed just the opposite of that hypothesized in Ref.5.

¹⁶Data taken from A. Ranfagni, G.P. Pazzi, P. Fabeni, G. Viliani, and M.P. Fontana, Solid State Commun. **14**, 1169 (1974); D. Mugnai, A. Ranfagni, O. Pilla, G. Viliani, and M. Montagna, *ibid.* **35**, 975 (1980).

¹⁷R. Englman, *The Jahn-Teller Effect in Molecules and Crystals* (Wiley-Interscience, London, 1972), p. 326.